

2015

Image similarity using dynamic time warping of fractal features

Ahmed Ibrahim

Security Research Institute, Edith Cowan University

Craig Valli

Security Research Institute, Edith Cowan University

Follow this and additional works at: <https://ro.ecu.edu.au/adf>



Part of the [Information Security Commons](#)

DOI: [10.4225/75/57b3fe44fb890](https://doi.org/10.4225/75/57b3fe44fb890)

13th Australian Digital Forensics Conference, held from the 30 November – 2 December, 2015 (pp. 111-122), Edith Cowan University Joondalup Campus, Perth, Western Australia.

This Conference Proceeding is posted at Research Online.

<https://ro.ecu.edu.au/adf/156>

IMAGE SIMILARITY USING DYNAMIC TIME WARPING OF FRACTAL FEATURES

Ahmed Ibrahim, Craig Valli
Security Research Institute, Edith Cowan University, Perth, Australia
aibrahi0@our.ecu.edu.au, c.valli@ecu.edu.au

Abstract

Hashing algorithms such as MD/SHA variants have been used for years by forensic investigators to look for known artefacts of interest such as malicious files. However, such hashing algorithms are not effective when their hashes change with the slightest alteration in the file. Fuzzy hashing overcame this limitation to a certain extent by providing a close enough measure for slight modifications. As such, image forensics is an essential part of any digital crime investigation, especially in cases involving child pornography. Unfortunately such hashing algorithms can be thwarted easily by operations as simple as saving the original file in a different image format. This paper introduces a novel technique for measuring image similarity using Dynamic Time Warping (DTW) of fractal features taken from the frequency domain. DTW has traditionally been used successfully for speech recognition. Our experiments have shown that it is also effective for measuring image similarity while tolerating minor modifications, which is currently not capable by state-of-the-art tools.

Keywords

Image Similarity, Dynamic Time Warping, Fuzzy Hashing, Perceptual Image Hashing

INTRODUCTION

Simple alteration to image files such as converting from one format to another (e.g. JPG to PNG) changes the file completely from a secure hashing point of view. Further modifications such as resizing, scaling or colour conversions leave hashing approaches helpless in identifying exact or close enough matches among images.

Applications of image matching include image retrieval, biometrics, medical diagnosis, video retrieval, detection of child pornography, and image forensics. The major theme discussed in this paper will be in the context of image forensics.

The state of the art for identifying images of interest in digital forensics comes down to a standard set of hashing techniques. Among the different approaches, MD5 and SHA-1 remain the predominant choices. They are ideal for assurance of file integrity. However, in certain applications, it is often necessary to identify similar files (e.g. Malware variants identification). Fuzzy hashing provides this ability as opposed to cryptographic hashing functions. This paper proposes an alternate approach that offers advantages over hashing approaches and through experimentation identifies where both approaches excel and fail.

As it would be demonstrated in this paper, simple operations on image files leave both traditional and fuzzy hashing techniques ineffective. The proposed approach is however, more robust in providing an acceptable match even when the image files have been altered.

This paper is divided into eight sections. The next section provides some background into related work that has been done in the domain of image similarity. This section is followed by technical details of the proposed approach on using DTW for image similarity. The next two sections outline the experimental designs and results for proposed approach and a fuzzy hashing tool. The section titled ‘Test of similarity’ will then evaluate the ability to measure image similarity among a sequence of related images using both the proposed and fuzzy hashing technique. The Discussion section then provides a detailed discussion of the results produced in the three previous sections, which leads to the conclusion of the paper.

BACKGROUND

MD5 and SHA variants uses cryptographic one-way hashing functions that are designed to have an “avalanche effect” (Rivest, 1992) when the source bits have the slightest changes. There have been several publications providing limitations of these hashing functions due to collision attacks (Hoffman & Schneier, 2005; Wang & Yu, 2005). However, MD5 and SHA variants are standard tools in the forensic investigator’s toolkit (Solomon, Rudolph, Tittel, Broom, & Barrett, 2011). MD5 and SHA-1 are the most common algorithms used to calculate

message digests in digital forensics (Casey, 2011). They are useful in matching identical files, however, they are not flexible enough to fulfil other use cases such as finding near identical or similar files.

The fuzzy hashing tool **ssdeep** (Fuzzy hashing and ssdeep, 2015) developed by Kornblum (2006) uses context triggered piecewise hashing (CTPH). The traditional piecewise hashing algorithm developed by Nicholas Harbour in 2002 and implemented as **dcfldd** (dcfldd, 2006), generates hashes for discrete fixed size segments instead of one single hash for the entire file. CTPH on the other hand uses a rolling hash, where the traditional hash is triggered based on the output of the rolling hash. The traditional hash is recorded in the CTPH signature and reset based on the rolling hash. Since CTPH signature is only partially dependant on the input, minor changes in the file are localized, thus enabling to match similar files with minor modifications (Kornblum, 2006). This ability to do partial matches can be useful in finding variants of the original object, e.g. Malware.

Similar to MD5 and SHA variants, ssdeep generates hashes at bit level of the file. As it would be demonstrated in Section 5, this is often ineffective when seeking similar images. Image similarity often warrants tools that are aware of the image content. Image and video indexing techniques used for content based image retrieval (CBIR) systems use a number of features such as colour, texture, shape, sketch, relationships among objects, to name but a few (Idris & Panchanathan, 1997). Discussing further on image retrieval is beyond the scope of this paper. A more detailed review can be found in Muller, Michoux, Bandon, and Geissbuhler (2004). Being aware of the image content offers advantages over bit-by-bit analysis in applications where some level of tolerance for alterations is required for practical reasons.

Perceptual image hashing (PIH) calculates the hash value based on features extracted from the image (Hadmi, Ouahman, Said, & Puech, 2012). According to Hadmi, et.al (2012) PIH could be classified as statistics, relation, coarse-representation, or low-level feature based schemes. An implementation of PIH is offered by Christoph Zauner as pHash (<http://www.phash.org/>), which implements DCT, Marr-Hildreth operator, radial variance, and block mean value based image hashing functions. It is robust against operations such as JPEG compression, rotation, and resize operations. (Zauner, 2010). Due to implementation issues in the test environment, we were unable to evaluate this tool along with ssdeep.

USING DTW FOR IMAGE SIMILARITY

DTW has gained popularity in the speech recognition (Sakoe & Chiba, 1978), and has been successfully applied in other areas such as data mining (Berndt & Clifford, 1994), gesture recognition (Arici, Celebi, Aydin, & Temiz, 2014), etc. A detailed review of DTW can be found in (Senin, 2008).

DTW algorithm is widely used for measuring similarity in times series in the presence of minor distortions in the time axis (Senin, 2008). It allows non-linear alignment of two similar time series that are locally out of phase (Ratanamahatana & Keogh, 2004).

As illustrated in Figure 1A, the Euclidean distance measures linearly between the i^{th} point of the reference sequence to the i^{th} point of the test sequence. This form of measurement produces inferior results compared to DTW, even though the two series are similar. DTW is able to non-linearly match (Figure 1B) and produce a more sophisticated similarity measure despite slight distortions (Keogh & Pazzani, 1999).

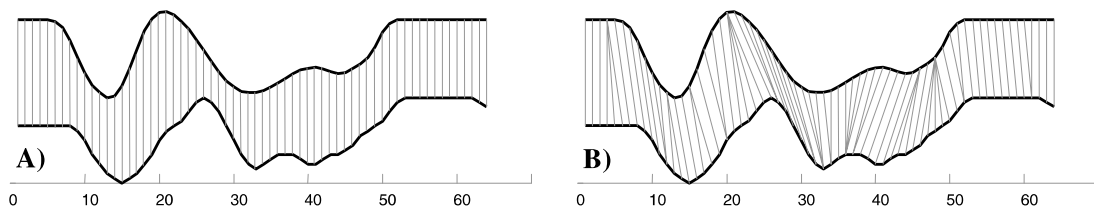


Figure 1: Euclidean linear (A) vs DTW non-linear (B) distance measurement (Keogh & Pazzani, 1999, p. 2)

DTW is a template-matching problem where a reference sequence R (known as the template) is matched to a test sequence T to measure the distance or similarity (Theodoridis & Koutroumbas, 2003). Suppose the reference and test sequences, are $R = \{r_1, r_2, \dots, r_N\}, N \in \mathbb{N}$ and $T = \{t_1, t_2, \dots, t_M\}, M \in \mathbb{N}$ respectively, DTW first constructs an $N \times M$ matrix where the (i^{th}, j^{th}) element is the distance between points r_i and t_j , represented as $d(r_i, t_j) = (r_i - t_j)^2$. A path through the matrix is obtained, which would minimize the warping cost given by

$$DTW(R, T) = \min \left\{ \sqrt{\sum_{k=1}^K w_k} \right.$$

















where w_k is the k^{th} element of the warping path W , i.e. $w_k = (i, j)_k$, in which W defines the mapping between R and T .

The sequences R and T are obtained by estimating the lacunarity of the quantised DCT (Q-DCT) coefficients of the reference and test images respectively. Lacunarity can be used to analyse distribution of gaps among a range of values at different scales to distinguish spatial patterns (Plotnick, Gardner, Hargrove, Prestegard, & Perlmutter, 1996). The Q-DCT coefficients, despite being from the frequency domain, can be treated similar to a texture of varying pixel values. Applications of lacunarity can be found in the medical and biological domains to investigate the multi-scaling fractal nature of natural textures (Barros Filho & Sobreira, 2008). Among the two most commonly used approaches, the Differential Box Counting (DBC) algorithm by Dong (2000) has been used in this paper due to its superiority to consider wider range of values as opposed to the Gliding Box (GB) algorithm by Allain and Cloitre (1991). For the purpose of this paper, instead of deriving the lacunarity of the whole sequence, a grid based approach of 8x8 windows has been used sequentially. Further details of Sequential Grid (SG) approach can be found in Ibrahim (2014).

EVALUATION OF DTW BASED IMAGE SIMILARITY IMPLEMENTATION

The datasets used are from the USC-SIPI image database (<http://sipi.usc.edu/database>), which consists of Aerials, Misc, Sequences, and Textures datasets. The following are some descriptions of the datasets.

Table 1: Sample images from all four datasets in the USC-SIPI database

Datasets	Sample Images			
Aerials 38 images (37 colour, 1 grayscale)				
Misc 44 images (16 colour, 28 grayscale)				
Sequences 69 images (all grayscale, 4 groups of sequences)				
Textures 64 images (all grayscale)				

The following four experiments were conducted to evaluate DTW for different scenarios of image similarity.

- **Experiment 1:** Compare same image in different image formats
- **Experiment 2:** Compare same image in different image formats of different colour models
- **Experiment 3:** Compare images at different scales
- **Experiment 4:** Comparison of image segments

Experiment 1: Compare same image in different image formats

The original TIFF images in all four datasets were first resized to 64x64 images (referred to as thumbnails henceforth). They were then converted to JPG, GIF, and PNG image formats. The reference images were then compared (Table 2) with the test images (R vs T) using the schemes; JPG vs PNG, JPG vs GIF, and PNG vs GIF. Since the reference and test sequences are based on Q-DCT coefficients, both PNG and GIF images were first pre-processing by converting to JPG before the comparison was made.

Table 2: DTW distance after comparison of same image in different image formats

Dataset	JPG vs PNG	JPG vs GIF	PNG vs GIF
Aerials	0	0.0267	0.0267
Misc	0	0.0097	0.0097
Sequences	0	0	0
Textures	0	0	0

Experiment 2: Compare same image in different formats of different colour models

The JPG thumbnails created in Experiment 1 were colour converted to grayscale. The initial thumbnail versions were then compared (Table 3) to the grayscale equivalent (R vs T) using the schemes JPG vs G-PNG, JPG vs G-GIF, and JPG vs G-JPG, where ‘G’ indicates grayscale.

Table 3: DTW distance after comparison of same image in different formats of different colour models

Dataset	JPG vs G-PNG	JPG vs G-GIF	JPG vs G-JPG
Aerials	1.1165	1.1207	1.1165
Misc	0.3753	0.3747	0.3753
Sequences	0.0002	0.0002	0.0002
Textures	0.0003	0.0003	0.0003

Experiment 3: Compare images at different scales

The Baboon and Jellybeans illustrated in Figure 2 in their original sizes (512x512 and 256x256 respectively) and thumbnail sizes (64x64 for both) are compared (Table 4) to the scaled down versions at 90%, 75%, 50%, and 25%. All images are compared after converting to grayscale.



(a) Baboon (512x512)



(b) Jellybeans (256x256)

Figure 2: (a) Baboon and (b) Jellybean used for comparison of resized images

Table 4: DTW distance after comparison of Baboon and Jellybeans resized at four different scales, Reference (R) images are the original (512x512, 256x256) and thumbnail (64x64)

Resize %	Baboon (512x512)	Jellybeans (256x256)	Baboon (64x64)	Jellybeans (64x64)
90%	0.3785	0.3259	0.0265	0.0279
75%	0.4681	0.4182	0.0202	0.0348
50%	0.7832	0.7361	0.0256	0.0427
25%	1.2985	1.2771	0.0512	0.0589

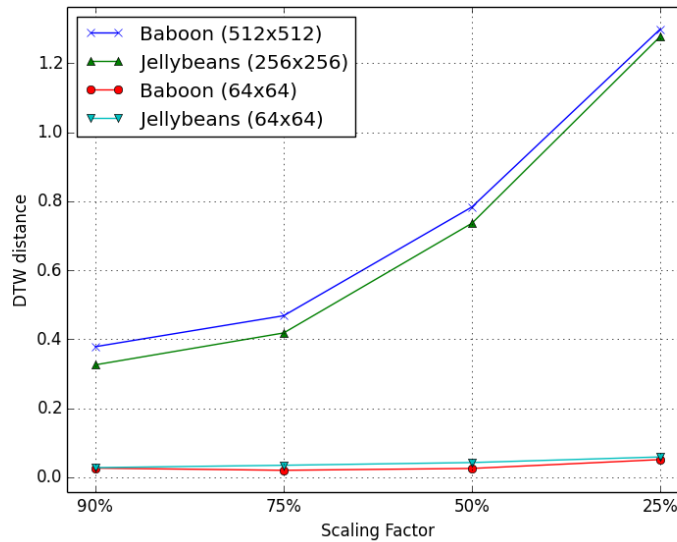
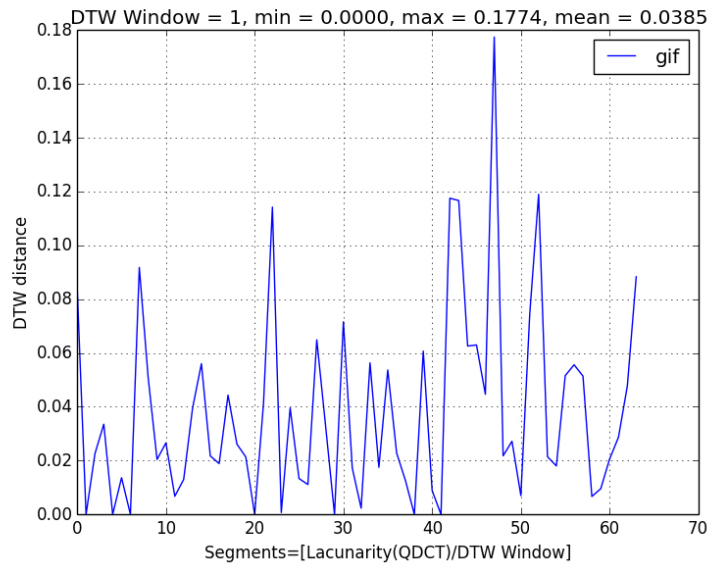


Figure 3: The trend shows that larger images tend to have significant increase in DTW distance (i.e. less similar) among scaled comparisons

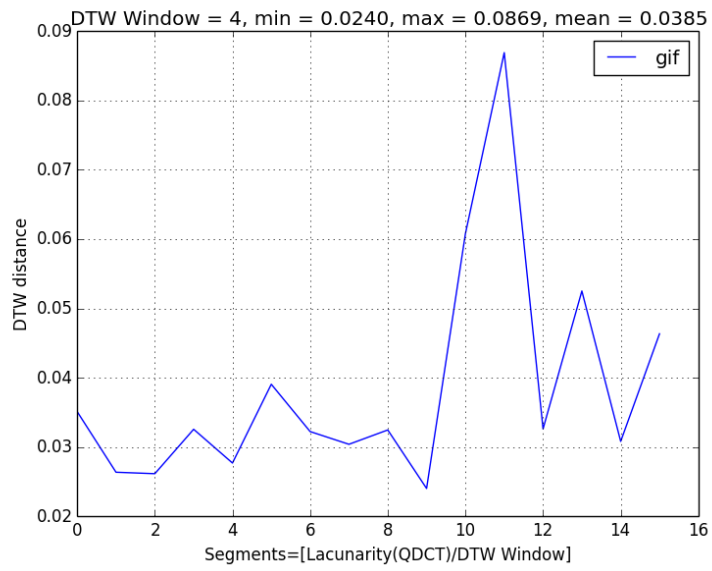
Experiment 4: Comparison of image segments

Segmented matching allows comparison of similarity among individual segments of an image rather than the whole image. Figure 4 shows comparison of JPG vs GIF of Baboon at different segmenting resolutions. The reference sequence (lacunarity measure of the Q-DCT coefficients) is compared individually to the corresponding segment in the test sequence. Segments are chosen based on a DTW windowing parameter. At window = 1, a single value is chosen from each sequence, which shows a fine resolution in the final DTW similarity distance (Figure 4a). At window = 4, each segment consists of 4 elements, thus a lower resolution sequence is produced (Figure 4b). However, regardless of the resolution, overall, both DTW distance sequences produced inhibit the same trend reflecting areas that are more similar (lower valleys) and areas that are less similar (higher peaks).

Figure 5a shows Baboon image with three segments highlighted (A,B,C). These regions were cropped, and individual segments were compared to the complete Baboon image, similar to a sliding window, starting from the top-left in a row wise manner. The window was slid, element-by-element, both horizontally and vertically. The heat maps shown in Figure 5b-5d show the projection of DTW distance values in two-dimensions. Dark regions indicate lower values (more similar) and bright regions indicate higher values (less similar) of DTW distance. Each sub-image in the figure is captioned with the minimum DTW distance value and location in the Baboon full sequence matrix that maps to the top-left element of the sliding window (i.e. the segment).

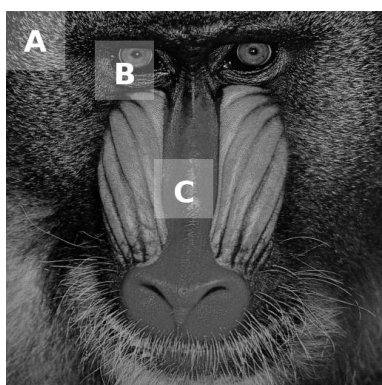


(a)

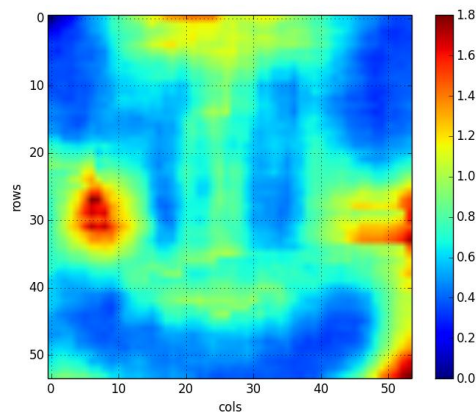


(b)

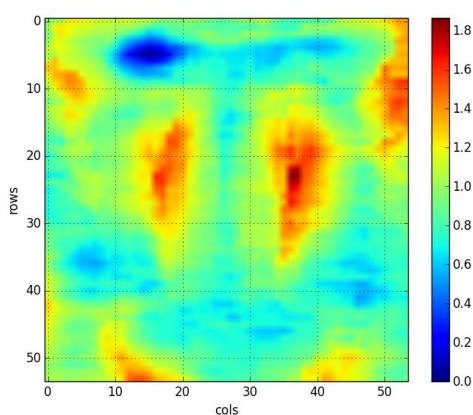
Figure 4: Comparison of image segments at different DTW windows (a) window=1 and (b) window=4



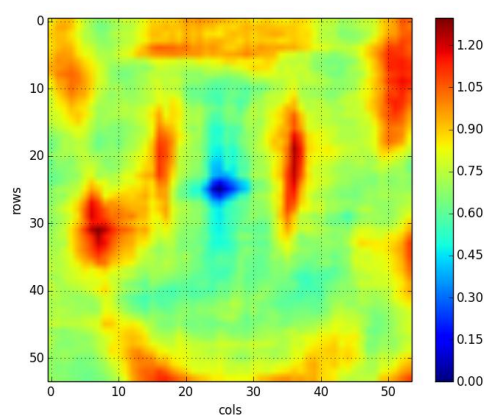
(a) Segments A,B,C



(b) $\min(\text{DTW distance}) = 0.0$
row = 0, col = 0



(c) $\min(\text{DTW distance}) = 0.0009$
row = 5, col = 15



(d) $\min(\text{DTW distance}) = 0.0$
row = 25, col = 25

Figure 5: (a) Baboon with segments A,B,C. (b-d) are 2D projections of DTW distances with $\min(\text{DTW distance})$, location of the match, and their respective colour bars indicating the scale of the DTW distance values. Sub-figures (b, c, d) correspond to segments A, B, C respectively. Darker regions indicate smaller distance, brighter regions indicate larger distances when their corresponding segment is overlapped and compared over the original image.

EVALUATION OF FUZZY HASHING ALGORITHM

The ssdeep tool is able to accept multiple options and parameters that can be adapted depending on the scenario. For the purpose of this section, ssdeep was executed with the “lrd” options with two folders to be compared as its parameters. An output is produced if similar files are found, indicating the matching file pair and also a similarity score, 100% being a perfect match. During the comparison, output is generated based on comparison among all input files. This means that in addition to inter-folder comparisons, it also performs intra-folder comparisons producing results that are not relevant for this task. Therefore, before evaluating the results, the outputs were pre-processed to remove all intra-folder comparisons to maintain the validity of the tests. Tables 5-7 list the results, where zero indicates no output. Where an output was generated, results have been presented in True Positive (TP)/False Positive (FP) format.

The following conditions were evaluated against all four datasets.

1. Comparison of different image formats
2. Comparison of different image formats after colour conversion to grayscale
3. Condition 1 and resize to 64x64
4. Condition 2 and resize to 64x64

Table 5: Images identified as similar under Conditions 1 and 2 are identical

Dataset	JPG vs PNG		JPG vs GIF		PNG vs GIF	
	Original	All JPG	Original	All JPG	Original	All JPG
Aerials (38)	0	38/0	0	1/0	0	1/0
Misc (44)	0	44/0	0	28/0	0	28/0
Sequences (69)	0	69/2	0	69/2	0	69/2
Textures (64)	0	64/0	0	64/0	0	64/0

Table 6: Images identified as similar under Condition 3, which are very similar to Table 5, except for Aerials and Textures datasets. Aerials dataset's FP has an average similarity score of 28%. Textures dataset's FP has an average similarity score of 30%.

Dataset	JPG vs PNG		JPG vs GIF		PNG vs GIF	
	Original	All JPG	Original	All JPG	Original	All JPG
Aerials (38)	0	38/0	0	4/32	0	1/0
Misc (44)	0	44/0	0	29/0	0	28/0
Sequences (69)	0	69/2	0	69/4	0	69/2
Textures (64)	0	64/0	0	51/49	0	64/0

Table 7: Images identified as similar under Condition 4, which are similar to Table 6, except for Aerials. Once again the Textures dataset's FP has an average similarity score of 30%.

Dataset	JPG vs PNG		JPG vs GIF		PNG vs GIF	
	Original	All JPG	Original	All JPG	Original	All JPG
Aerials (38)	0	38/0	0	1/1	0	1/0
Misc (44)	0	44/0	0	29/0	0	28/0
Sequences (69)	0	69/2	0	69/4	0	69/2
Textures (64)	0	64/0	0	51/49	0	64/0

TEST OF SIMILARITY

The previous two sections presented the evaluation of DTW based image similarity implementation and fuzzy hash algorithms individually. This section will assess both approaches comparatively for similarity measure.

To test the similarity, the 64x64 grayscale Sequences dataset was chosen and subdivided into the four groups (Sequence 1,2,3,4) of sequences. Each sequence subset is a series of frames captured from a short movie clip with varying number of frames per subset. Figure 6 shows the beginning and ending frame of each sequence. The first image of each sequence was used as the reference image and the rest of the images were used as the test images where the comparison was made one-by-one. The results have been plotted in Figure 7. The smallest DTW distance indicating the most similar image for all sequences have been observed as the first image that followed the reference image. Table 8 lists the min, max, and mean for the DTW distance for each sequence. The fuzzy hash tool was unable to produce any matches from any sequence.

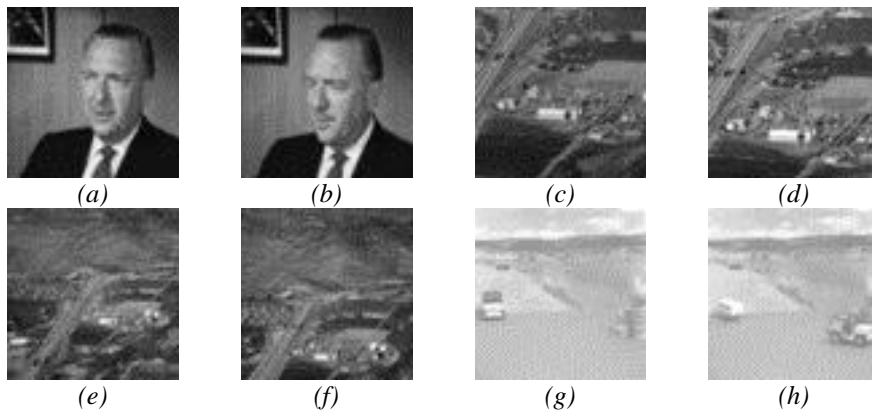


Figure 6: (a-b) Sequence 1: 16 frames, (c-d) Sequence 2: 32 frames, (e-f) Sequence 3: 11 frames, and (g-h) Sequence 4: 10 frames

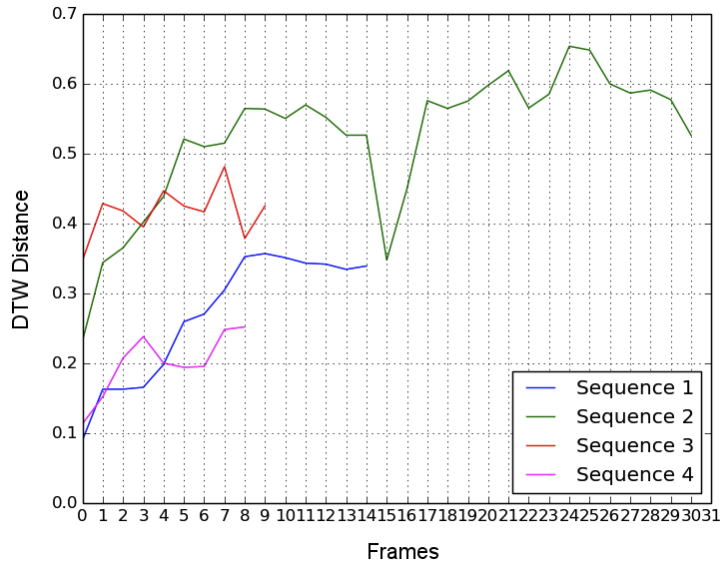


Figure 7: Plot of all DTW distances in each sequence between the reference image and all test images per sequence

Table 8: Summary of all DTW distances in each sequence

Subset	Min	Max	Mean
Sequence 1	0.0897	0.3567	0.2687
Sequence 2	0.2318	0.6534	0.5238
Sequence 3	0.3470	0.4811	0.4160
Sequence 4	0.1130	0.2517	0.1999

DISCUSSION

The experiments presented in the evaluation of DTW implementation attempted to ascertain its robustness and applicability to compare four image datasets while basic image operations were carried out on the image file. Such operations alter the cryptographic hashes of the images significantly.

The DTW based approach uses lacunarity estimates derived from Q-DCT coefficients. Lacunarity estimate is able to measure fractal properties of the Q-DCT coefficients, and in combination with resizing the image to 64x64 pixels, the number of features are significantly reduced while maintaining the nature of the data. Since DTW is computationally expensive (Keogh & Pazzani, 1999), this feature reduction is essential for practicality.

From Experiment 1, the mean values indicate that most of the dataset have a DTW distance of zero or mean value close to zero. Experiment 2 did the same comparison, however all images were subject to colour conversion to grayscale. The results show that Sequences and Textures datasets as being very similar. However, the larger distance values in Aerials and Misc datasets reveal the reason for the DTW distance of the former to be significantly smaller. As per the original dataset, both Sequences and Textures datasets were already in grayscale mode. Whereas about one third of the Misc dataset and almost all of the Aerials dataset were in colour. Thus the colour conversion had a more significant effect on the reproduced grayscale images that were used for this experiment.

Comparing two different lengths of reference and test sequences using DTW distance measure is not preferred (Ratanamahatana & Keogh, 2004), however, the results indicate an interesting trend. The two candidate images, Baboon and Jellybean, were resized at 90%, 75%, 50%, and 25%. Two different origin sizes for both images were used. Figure 3 indicates that larger images had a much severe effect when resized, inhibiting a large DTW distance. Thus, one can observe scaling operations can be tolerated more when dealing with smaller images, which re-enforces the premise for scaling all images to 64x64 in the beginning of Experiment 1.

Aside from image format conversion and colour conversion, cropping is also a common operation applied for image storage. Furthermore, it is also not uncommon to retrieve fragments of image files during digital evidence acquisition. Construction of image fragments is a broad topic and is beyond the scope of this paper. However, in

a scenario where only a portion of an image is available, segmented matching can be useful. Figure 4a and 4b shows a comparison of individual segments between Baboon.jpg and Baboon.gif. It can be observed that different segments have different levels of similarity. From Table 2, it can be seen that comparing JPG and GIF images have a high degree of similarity. However, it also depends on the nature of the image, which is also shown in Figure 4. At different windowing resolutions, the DTW distance have a mean of 0.0385. This is comparatively close enough to the values in Table 2. A comparison of JPG and PNG was not presented because DTW based similarity measure between Baboon.jpg and Baboon.png revealed to be identical in the segmented match.

Based on the segmented matching technique, a smaller reference image (cropped segment, or recovered fragment) can be compared to a whole image in a sliding window manner to identify the location with the highest similarity. Figures 5b-5d show that the segmented matching can identify the exact match with the least DTW distance.

Based on the Experiments 1-4, the following observations can be made regarding the proposed approach.

1. Similar images can be identified even when they have been converted to different image formats.
2. Converting from colour to grayscale has a significant effect on the similarity measure.
3. Similarity measure among smaller images are more tolerant to image scaling.
4. Segmented matching can identify segment location from the larger image.

Evaluation of fuzzy hashing tool, ssdeep, reveals interesting results among the different datasets. Two general conditions were tested during the evaluation, i.e. to see the effect of image format conversion, and also the effect of colour conversion. These two conditions were tested in different sizes, the respective datasets' original size, and rescaling the images to 64x64 thumbnails, similar to the pre-processing in the proposed approach.

Two significant observations can be made from the results. The first being, ssdeep was unable to identify any similar matches when different file formats were compared, i.e. JPG with PNG, JPG with GIF, and PNG with GIF. However, when all the images were converted to JPG format as a pre-processing step, it was able to identify similarities.

The second observation is that pre-processing PNG and GIF to JPG produces better similarity results. Following the pre-processing to JPG, it can be observed that despite being the same dataset, similarity among different file formats were inconsistent. The Misc and Sequences dataset remained the most consistent throughout the different conditional tests. The Aerials and Textures datasets produced significant False Positives when resized to 64x64 among the JPG vs GIF comparison.

Furthermore, even though both GIF and PNG are lossless image formats, the results show that both have different similarity results during the comparison. PNG images retained more similarity at a bit level compared to GIF.

Lastly, a comparison was made between the proposed approach and ssdeep. We would like to note that, while both approaches are significantly different in design; i.e. DTW based similarity measure being more closely related to PIH and ssdeep relying on bit-level hashing; it is useful to evaluate their ability to measure similarity among images that are perceived to be similar. Thus, contiguous frames in different sequences were compared to the first frame of each sequence. The fuzzy hashing tool was unable to identify any similar images. The DTW distance values obtained from the proposed approach plotted in Figure 7 reveals that the most similar image in all the sequences was the second frame in each sequence. However, different sequences had different magnitudes of similarity, and different mean values as shown in Table 8. In order to make a comparison of success or failure, we would need to set a threshold that can be universally applied to all scenarios. It is unfortunately not trivial, as it has been discussed thus far, a number of variables affect the similarity measure even when the same image is compared to its variants. Furthermore, it has also been observed that different datasets produce different similarity measures under the same conditions. Thus, a threshold is yet to be determined in future research.

CONCLUSION

This paper has proposed the application of Dynamic Time Warping (DTW) using lacunarity estimates of quantised DCT (Q-DCT) coefficients to check image similarity. This approach is contrasted with fuzzy hashing, where the hashing approach is more tolerant to slight alterations at a bit-level compared to traditional

cryptographic hash functions such as MD5 and SHA-1. However, the results reveal that, simple image operations such as conversion of image format produces enough alterations at the bit-level that hinders fuzzy hash to identify the same image in different formats. The proposed DTW based approach is able overcome such operations and produces significantly better results.

While the same cannot be mentioned for other operations such a colour conversion and rescaling, the segmented matching is able to identify matching regions of smaller segments against its full image. This is useful in forensic applications in scenarios where image fragments have been recovered.

The overall results, including the evaluation of similarity among similar image sequences reveals that further work needs to be done to identify a universal threshold value that can cater for different scenarios and different image content.

The experimental results based on four different datasets under different conditions reveals that the proposed DTW based image similarity approach has advantages over traditional hashing approaches under certain conditions. Further research would be done to explore avenues for improvement.

REFERENCES

- Allain, C., & Cloitre, M. (1991). Characterizing the lacunarity of random and deterministic fractal sets. *Physical review*, 44(6), 3552.
- Arici, T., Celebi, S., Aydin, A. S., & Temiz, T. T. (2014). Robust gesture recognition using feature pre-processing and weighted dynamic time warping. *Multimedia Tools and Applications* , 72 (3), 3045-3062.
- Barros Filho, M. N. & Sobreira, F. J. A. (2008). Accuracy of lacunarity algorithms in texture classification of high spatial resolution images from urban areas. In *XXI Congress of International Society of Photogrammetry and Remote Sensing*.
- Berndt, D. J., & Clifford, J. (1994). Using Dynamic Time Warping to Find Patterns in Time Series. *KDD workshop* , 10 (16), 359-370.
- Casey, E. (2011). *Digital evidence and computer crime: Forensic science, computers, and the internet*. Elsevier Science.
- Dong, P. (2000). Test of a new lacunarity estimation method for image texture analysis. *International Journal of Remote Sensing*, 21(17), 3369-3373.
- dcfldd. (2006). From <http://dcfldd.sourceforge.net/>
- Fuzzy hasing and ssdeep. (2015). Retrieved September 27, 2015 from <http://ssdeep.sourceforge.net/>
- Hadmi, A., Ouahman, A. A., Said, B. A., & Puech, W. (2012). *Perceptual image hashing*. INTECH Open Access Publisher.
- Hoffman, P., & Schneier, B. (2005). Attacks on cryptographic hashes in Internet protocols. RFC No. 4270 .
- Ibrahim, A. (2014). Suitability of lacunarity measure for blind steganalysis. *Proceedings of the 12th Australian Digital Forensics Conference*.
- Idris, F., & Panchanathan, S. (1997). Review of image and video indexing techniques. *Journal of visual communication and image representation* , 8 (2), 146-166.
- Keogh, E. J., & Pazzani, M. J. (1999). Scaling up dynamic time warping to massive datasets. *Principles of Data Mining and Knowledge Discovery* , 1-11.
- Kornblum, J. (2006). Identifying almost identical files using context triggered piecewise hashing. *Digital investigation* , 3, 91-97.
- Morgan, D., & Scofield, C. (1991). *Neural networks and speech recognition*. Boston: Kluwer Academic Publishers.
- Muller, H., Michoux, N., Bandon, D., & Geissbuhler, A. (2004). A review of content-based image retrieval systems in medical applications—clinical benefits and future directions. *International journal of medical informatics* , 73 (1), 1-23.

- Plotnick, R. E., Gardner, R. H., Hargrove, W. W., Prestegaard, K., & Perlmutter, M. (1996). Lacunarity analysis: a general technique for the analysis of spatial patterns. *Physical review E*, 53(5), 5461.
- Ratanamahatana, C., & Keogh, E. (2004). Everything you know about dynamic time warping is wrong. Third Workshop on Mining Temporal and Sequential Data.
- Rivest, R. (1992). The MD5 message-digest algorithm.
- Sakoe, H., & Chiba, S. (1978). Dynamic programming algorithm optimization for spoken word recognition. *IEEE Transactions on Acoustics, Speech and Signal Processing*, 26 (1), 43-49.
- Senin, P. (2008). Dynamic time warping algorithm review. University of Hawaii .
- Solomon, M. G., Rudolph, K., Tittel, E., Broom, N., & Barrett, D. (2011). *Computer forensics jumpstart*. John Wiley & Sons.
- Theodoridis, S., & Koutroumbas, K. (2003). *Pattern recognition (2nd Edition ed.)*. Amsterdam: Academic Press.
- Wang, X., & Yu, H. (2005). How to break MD5 and other hash functions. In *Advances in Cryptology - EUROCRYPT 2005* (pp. 19-35). Springer.
- Zauner, C. (2010). *Implementation and benchmarking of perceptual image hash functions* (Master's thesis, University of Applied Sciences, Upper Austria, Austria).